

Laser Safety ibeo NEXT

Release information

	Surname	First name	Process role	Date
Responsible	Schneider	Georg	Laser safety manager	
Reviewer	Kiehn	Michael	Laser safety officer	January 17, 2019
Reviewer	Bendt	Jürgen	Developer (INLD)	April 3, 2019
Reviewer	Diebel	Falko	Developer (INRA)	
Reviewer	Gorris	Friederike	Developer (INVCSEL)	
Reviewer	Hölling	Andy	Developer (Optics)	
Reviewer	Houalef	Sid	Functional safety manager	
Reviewer	Keye	Christoph	Developer (Architecture)	
Reviewer	Montavani	Federico	Developer (INLD)	
Reviewer	Schulmeister	Karl	External Laser Safety Expert	

Change history

Date	Version	Change description	Author	Status
June 22, 2019	1.3	<ul style="list-style-type: none">• updated references• included abbreviations• minor text corrections• added 32° optic• added more detailed descriptions• added high resolution advanced evaluation	GeS	in progress

Date	Version	Change description	Author	Status
March 29, 2019	1.2	<ul style="list-style-type: none"> • updated the INLD requirements according to specification • added detailed description for safety assurance for different samples • included a full analysis for arbitrary accommodation states • changed temporal analysis to 1nJ • updated VCSEL divergence to 6.7° • added discussion about closest point of human access • updated example calculation to 11.2° 	GeS	reviewed
January 22, 2019	1.1	<ul style="list-style-type: none"> • clarified reference point definition • added document references • added details about VCSEL power 	GeS	released
January 16, 2019	1.0	first draft	GeS	reviewed

Contents

i	Index of Abbreviations and Terms	4
ii	References and Documents	4
iii	Index of Figures	4
iv	Index of Tables	5
1	Scope	6
2	ibeo NEXT LiDAR description	6
2.1	Emitter parameters	6
2.2	Optics parameters	8
3	Laser class 1 analysis	9
3.1	Norm parameters	9
3.2	Measurement condition	11
3.3	Norm criteria	11
3.4	Simplified Analysis (accommodation to infinity)	12
3.4.1	Image analysis	12
3.4.2	Temporal analysis	14
3.5	Advanced analysis (arbitrary accommodation & row order)	16
3.5.1	Image analysis	17
3.5.2	Temporal analysis	18
3.6	Configuration parameters	19
4	Single-fault condition	20
4.1	Critical parameters	20
4.2	Component requirements	21
4.2.1	INLD	21
4.2.2	INRA	22
4.3	Safety Assurance	23
4.3.1	Pulse power	23
4.3.2	Pulse width	25
4.3.3	Row sequence	25
4.3.4	Time between shots	25
4.3.5	Configuration	26
5	Hazard analysis	26
5.1	Closest point of human access	26

i Index of Abbreviations and Terms

Abbreviation	Definition
AE	accessible emission
AEL	accessible emission limit
INLD	ibeo NEXT Laser Driver
INRA	Ibeo NEXT Receiver ASIC
LMU	Laser Monitoring Unit
MHP	Most Hazardous Position
VCSEL	Vertical-Cavity Surface-Emitting Laser

ii References and Documents

- [1] DIN EN 60825-1:2015-07. *Sicherheit von Lasereinrichtungen – Teil 1: Klassifizierung von Anlagen und Anforderungen (IEC 60825:2014).*
- [2] AMS Communication. *190121 - IBERIA - Short Pulse Data - updated.pdf.*
- [3] F. Gorris. *190110-LIV-calc-VCSEL Power.xlsx.*
- [4] *FLT-FE-200000_SensorHeadVariants (v1.6). (PTC).*
- [5] IEC 60825-1:2014/ISH1:2017. *Interpretation sheet 1 – Safety of laser products – Part1: Equipment classification and requirements (2017). (IEC Webstore).*
- [6] *REQ-FE-300004 INLD (v1.16). (PTC).*
- [7] *INLD_A0_ErrataSheet_V1.6.4-call20181220 (v1.1). (PTC).*
- [8] *INRA Digital Design Spec (v1.3.2.22). (PTC).*
- [9] *REQ-FE-300005_VCSEL Array - B - 3-stack (CC) (v1.8). (PTC).*

iii Index of Figures

Fig. 1	Emitter geometry	6
Fig. 2	VCSEL energy as a function of temperature	7
Fig. 3	Relative VCSEL power	8
Fig. 4	Position of the exit pupil used as reference point	11
Fig. 5	Image Analysis for all optics	14
Fig. 6	Simplified analysis for all optics	15

Fig. 7	Result of an advanced image analysis	17
Fig. 8	Comparison between simplified and advanced analysis	18
Fig. 9	Sensor safety margins for closest point of human access	26

iv Index of Tables

Tab. 1	Emitter parameters and use case definition	7
Tab. 2	Optics parameters	8
Tab. 3	Angular subtense and angular VCSEL spacing	13
Tab. 4	Result of image analysis	13
Tab. 5	Configuration conditions	19

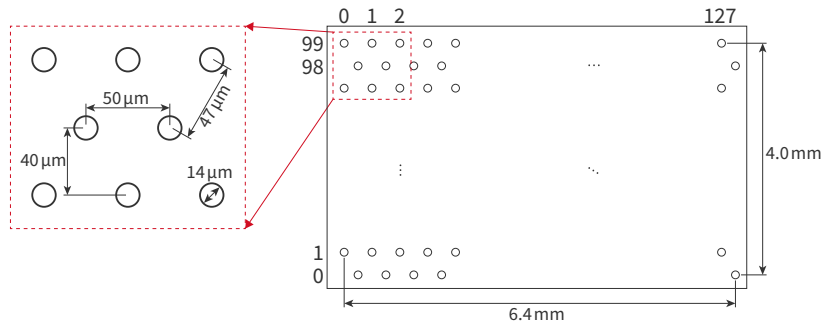


Fig. 1: The emitter geometry consists of an array of 128×100 single emitters.

1 Scope

The scope of this work is the classification of the ibeo NEXT LiDAR system according to the official standard [1]. The system consists of different hardware components and software configurations which will be introduced throughout this document. Furthermore, the document discusses single point of failure conditions and mechanisms to ensure safe operation.

2 ibeo NEXT LiDAR description

2.1 Emitter parameters

The geometry of the emitter unit is shown in figure 1. Single VCSELs are distributed over 100 rows and 128 columns and form an array with a total width of about 6.4 mm and 4.0 mm height. The horizontal spacing between two adjacent emitters is $d_H = 50 \mu\text{m}$ and $d_V = 40 \mu\text{m}$ between two adjacent rows. In addition, each second row has a horizontal offset of $\pm 25 \mu\text{m}$ relative to the one before, as shown in the figure, such that nearly isosceles triangles are formed. All VCSELs have a diameter of $d_{\text{VCSEL}} = 14 \mu\text{m}$ and emit laser light at $\lambda = 885 \text{ nm}$ with a beam divergence¹ of $\theta = 6.7^\circ$ [2] (FWHM) and an intensity profile which shall be approximated by a Gaussian shape. The actual pulse has a broader distribution than a Gaussian profile, which makes the analysis more restrictive.

Typically, only 80 of the 100 rows are operated which is realized by two different wiring configurations. In configuration 1 the central 80 rows are operated and the 10 rows on the top and on the bottom are not operational. In the second configuration the central 60 rows are operational and each second from the remaining 20 on the top and on the bottom. Configuration 1 is the standard configuration.

The VCSEL array is operated row-wise, which means that all emitters of one row fire at the same time for n_{shot} times with a period between shots of T_{shot} and an energy of $E_{\text{pulse}} = P_{\text{pulse}} \times t_{\text{pulse}}$. Once this shot sequence (or *burst*) is finished for one row, the row stops emitting light and another row starts the next sequence, however, only one row is active at the a time. The row order is customizable (e.g. 20–64–75–27...) and not necessarily in

¹The value is based on a measured divergence for an emission time of $100 \mu\text{s}$ with a similar VCSEL. It is expected that the divergence at the design configuration is θ or smaller. In particular, the beam divergence is not necessarily constant for different emission times due to different modes.

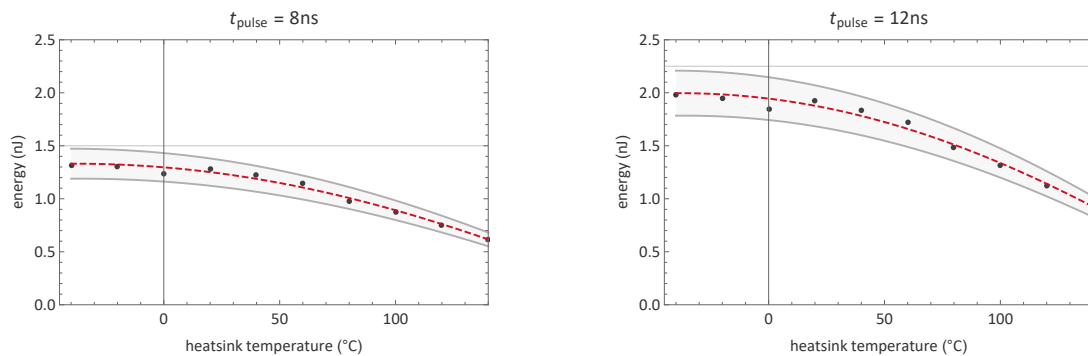


Fig. 2: The plot shows the VCSEL energy as a function of the heatsink temperature [3] for a pulse width of 8 ns (left) and 12 ns (right) at 6A. The dashed line is a heuristic second order polynomial fit to the measured data. The gray bands indicate a $\pm 10\%$ tolerance on the current. The worst case achievable pulse energy for randomly chosen sample is 1.5 nJ at 8 ns and 2.3 nJ at 12 ns, respectively.

sequential order (e.g. 1-2-3-4...).

Typically, a burst of one row requires a time of $T_{\text{row}} = 500 \mu\text{s} = (n_{\text{shot}} - 1) T_{\text{shot}}$ such that the time to fire one burst with all rows matches $T_{\text{frame}} = 40 \text{ ms} = 80 T_{\text{row}}$, which is defined as one *frame* based on an adjustable frame rate of $f_{\text{frame}} = 25 \text{ Hz}$. In the case that a burst is finished before 500 μs or a frame is finished before 40 ms a short pause is included to ensure that the 25 frames exactly match an emission time of $t_{\text{emiss}} = 1 \text{ s}$.

The timing for one frame is a fixed parameter depending on the frame rate, while the timing for a single row can vary from row to row depending on the system configuration ($\sum_{i=1}^{80} T_{\text{row}}^{(i)} = 40 \text{ ms}$). Table 1 summarizes the emitter parameters and defines the standard use case configurations for the sensor. The pulse energy is set to 1 nJ for the calculation. shown in figure 2. It is important to note that the pulse energy is not constant under all operation conditions, see figure 2. The figure shows, that the energy per shot is a function of the sensor temperature. This impact will be discussed in more detail, when the actual pulse energies are calculated, see section 3.6.

Parameter	Symbol	Unit	I	II	III
wavelength	λ	nm	885		
pulse energy (normalized)	E_{pulse}	nJ	1		
pulse width (typical)	t_{pulse}	ns	8		
number of shots (maximal)	n_{shot}	1	374	749	936
shot period	T_{shot}	μs	1.334	0.667	0.534
burst period	T_{burst}	μs	500	500	500

Tab. 1: Emitter parameter and use case definition. The pulse energy is set to exactly 1 nJ for the calculation only, the actual value for the final configuration is adjusted based on the laser safety result. The number of shots is the maximum number of shots that fits in one burst based on the shot period. In the actual sensor configuration the number of shots will always be lower than this number if all rows are fired for the same amount of time.

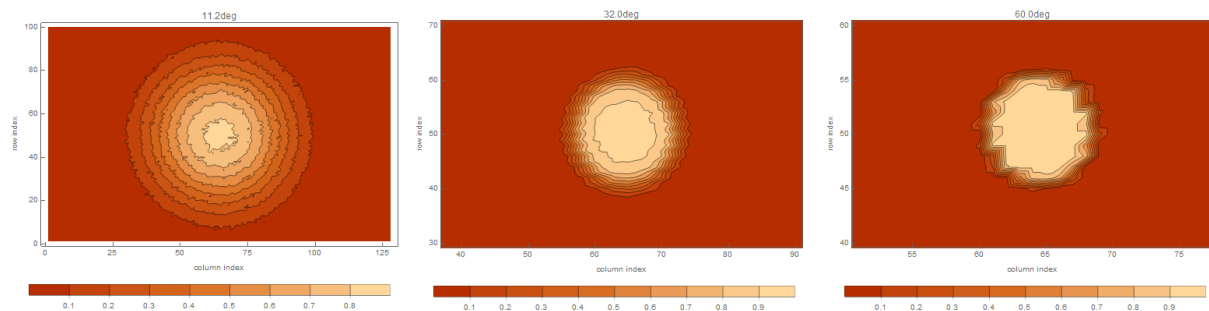


Fig. 3: Relative VCSEL power for all optics through a 7 mm aperture at 100 mm distance for each individual VCSEL emitter. The axes are based on the VCSEL index coordinates. For example the central VCSEL with coordinates (64,50) enters the eye with about 90% of its total power in the case of the 11° optics, while in the case of 60° the total power is about 100%. Note the different zoom levels in the plot range from left to right.

2.2 Optics parameters

The VCSEL array, as defined above, is placed in the focal plane of an optics. Typically, the optics consists of multiple lenses but shall be treated as one effective lens with focal length f_0 and aperture diameter D_0 . Table 2 shows the optics parameters [4] for three different configurations which are directly related to the use cases of the previous section.

The table also includes an analysis of the relative power $P_{rel} = P_{detected}/P_{pulse}$ that enters a $D_{Eye} = 7$ mm aperture at a distance of 10 cm. The analysis is based on an OpticsStudio simulation which includes the full geometry of the optics, and was performed for the central VCSEL as well as for all VCSELs of the array (128 × 100). At this distance and aperture all VCSELs of the 11.2° sensor contribute to the received power at least partially, refer to figure 3. For the larger field of views the light emitted from VCSELs on the edges does not enter the 7 mm aperture anymore.

Parameter	Symbol	Unit	I	II	III
focal length	f_0	mm	32.6	11.3	5.5
f-Number	N_0	1	2.0	1.1	1.1
aperture diameter	D_0	mm	16.3	10.3	5.0
field-of-view	$\Phi_H \times \Phi_V$	°	11.2 × 5.6	32 × 16	60 × 30
relative power central VCSEL 10 cm distance with 7 mm aperture	P_{rel}	1	0.30	0.78	0.86
relative power all VCSELs 10 cm distance with 7 mm aperture	P_{rel}	1	0.097	0.011	0.0035

Tab. 2: Optics parameters for three different field of views. 'H' refers to the horizontal field-of-view and 'V' to the vertical. The first relative power refers to the ratio of the emitted power of the central VCSEL compared to the power that actually enters the eye. The second relative power refers to the ratio of the total emitted power of the whole array compared to the power that enters the eye.

3 Laser class 1 analysis

The analysis in this section is based on the official standard [1]. First, the relevant parameters are introduced and evaluated for the ibeo NEXT LiDAR sensor. In the next step the norm criteria are evaluated for all possible emission times and optics/use cases.

3.1 Norm parameters

This section summarizes the main parameters for the laser safety evaluation.

- **Time base**

The time base for the analysis is set to 100s, because “intentional long-term viewing” is not “inherent in the design or function of the laser product”.

- T_i

T_i defines the time below which pulse groups are summed and treated as one effective pulse. For the design wavelength in the range $400 \text{ nm} \leq \lambda < 1050 \text{ nm}$ the time is set to $T_i = 5 \mu\text{s}$. The physical background is the thermal diffusion time in the eye.

- **Angular subtense of the apparent source**

The minimal angular subtense of an image on the retina is defined as $\alpha_{\min} = 1.5 \text{ mrad}$. The maximum angular subtense α_{\max} , on the other hand, is emission time dependent

$$\alpha_{\max}(t) = \begin{cases} 5 \text{ mrad} & t < 625 \mu\text{s} \\ 200\sqrt{t} \text{ mrad} & 625 \mu\text{s} \leq t \leq 0.25 \text{ s} \\ 100 \text{ mrad} & 0.25 \text{ s} < t \end{cases} \quad (1)$$

where t is dimensionless. The larger the image on the retina the longer it takes to cool the center of the spot. However, at a certain size the spot does not become more dangerous, because the spot is now larger than the typical diffusion length, and the center is not affected by the cooling on the spot boundary. In other words, the maximum temperature in the center will not increase further for larger spots

- T_2

The time T_2 accounts for eye movement and depends on the angular subtense of the image. The larger the spot the more eye movement would be necessary to achieve disjoint spots on the retina.

$$T_2 = \begin{cases} 10 \text{ s} & \alpha \leq 1.5 \text{ mrad} \\ 10 \text{ s} \times 10^{\frac{\alpha - 1.5 \text{ mrad}}{98.5 \text{ mrad}}} & 1.5 \text{ mrad} < \alpha \leq 100 \text{ mrad} \\ 100 \text{ s} & 100 \text{ mrad} < \alpha \end{cases} \quad (2)$$

- C_4

This correction factor models the change of absorbance in the Melanin layer of the eye depending on the wavelength.

$$C_4 = 10^{2 \cdot 10^6 (\lambda - 700 \text{ nm})} \Big|_{\lambda=885 \text{ nm}} = 2.34 \quad (3)$$

- C_5

This correction factor models the dependence of the limits for multiple pulses. The correction factor is only applied to pulses with an emission time $t_{\text{emiss}} < 0.25\text{s}$. In addition, two cases have to be distinguished. If the pulse duration t (or group duration of several pulses) is smaller than T_i the micro cavitation correction factor has to be applied

$$C_5 = \begin{cases} 1 & N \leq 600 \\ \max(5N^{-0.25}, 0.4) & N > 600 \end{cases} \quad (4)$$

while for longer durations $t > T_i$ the thermal correction factor must be used

$$C_5 = \begin{cases} 1 & \alpha^* \leq 5 \text{ mrad} \\ \begin{cases} N^{-0.25} & N \leq 40 \\ 0.4 & N > 40 \end{cases} & 5 \text{ mrad} < \alpha^* \leq \alpha_{\text{max}} \\ \begin{cases} N^{-0.25} & N \leq 625 \\ 0.2 & N > 625 \end{cases} & \alpha_{\text{max}} < \alpha^* \leq 100 \text{ mrad} \\ 1 & 100 \text{ mrad} < \alpha^* \end{cases} \quad (5)$$

Here, N is defined as the number of group durations during T_2 or t_{base} whichever is shorter. Thus, the number of effective pulses can be calculated by

$$N = \left\lfloor \frac{\min(T_2, t_{\text{base}})}{t} \right\rfloor + 1 \quad \text{and} \quad N_{\text{max}} = \left\lfloor \frac{\min(T_2, t_{\text{base}})}{T_i} \right\rfloor + 1, \quad (6)$$

where the brackets $\lfloor \rfloor$ indicate that the resulting number is rounded to the next lower integer. α^* refers to the angular subtense of an image analysis which was performed without a limit for α_{max} . In contrast α is restricted to the time dependent value of $\alpha_{\text{max}}(t)$.

- C_6

This correction factor accounts for an extended source and increases the emission limits.

$$C_6 = \begin{cases} 1 & \alpha \leq \alpha_{\text{min}} \\ \alpha / \alpha_{\text{min}} & \alpha_{\text{min}} < \alpha \leq \alpha_{\text{max}} \\ \alpha_{\text{max}} / \alpha_{\text{min}} & \alpha_{\text{max}} < \alpha \end{cases} \quad (7)$$

- E_{AEL}

The accessible emission limit for a laser class 1 extended source in the wavelength range $700\text{nm} < \lambda \leq 1050\text{nm}$ is

$$E_{\text{AEL}} = \begin{cases} 3.8 \times 10^{-8} C_6 \text{ J} & 10^{-13} < t \leq 10^{-11} \\ 7.7 \times 10^{-8} C_4 C_6 \text{ J} & 10^{-11} < t \leq 5 \times 10^{-6} \\ 7 \times 10^{-4} t^{3/4} C_4 C_6 \text{ J} & 5 \times 10^{-6} < t \leq T_2 \\ 7 \times 10^{-4} T_2^{-1/4} t C_4 C_6 \text{ J} & T_2 < t \end{cases} \quad (8)$$

where all times are unitless.

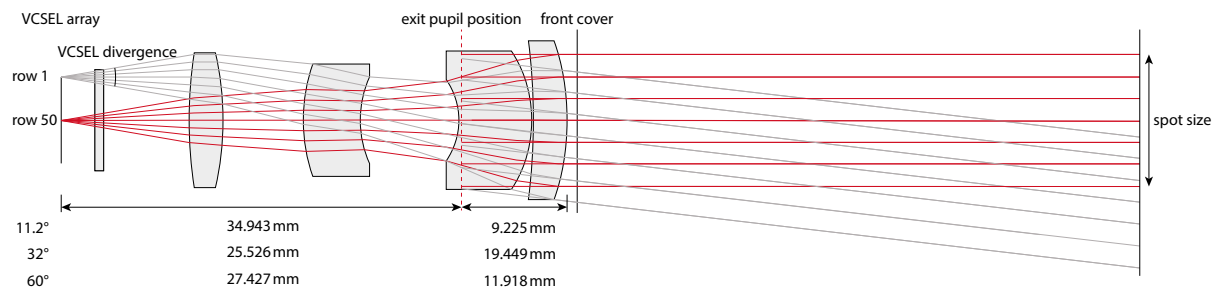


Fig. 4: Geometry of the exit pupil for the 11.2° optic relative to the position of the VCSEL array, which is used as the reference point for the laser safety analysis. The position is determined by a ZEMAX OpticStudio simulation.

3.2 Measurement condition

The ibeo NEXT LiDAR system is operated in the retinal hazard region 400 nm to 1400 nm. Further evaluation will show, that the system represents an extended, pulsed and scanning source. Thus, the measurement condition has to consider the most restrictive region by varying the spatial measurement position (x, y and z), variation of the eye accommodation, and variation of the relevant image size for each emission time.

The minimal distance which has to be considered is 100 mm from the reference point with an aperture of 7 mm for condition 3 [1]. The reference point for a scanner or scan-like device is defined as the pivot point. For the actual analysis the reference point is set to the position of the exit pupil. Based on the actual optics setup the position of the reference point relative to the VCSEL array is 34.943 mm, 25.526 mm and 27.427 mm for 11.2°, 32° and 60°, as shown in figure 4. Note, that these values cannot be used in the effective lens model.

Condition 1 (telescope condition) needs not to be considered for scanning laser systems. In addition, condition 2 (loupe criterion) from the earlier standard ed. 2 is already included in condition 3 of ed. 3.

3.3 Norm criteria

Based on the system description the sensor must be treated as a repetitively irregular pulsed, extended and scanning source at constant wavelength. The standard gives three requirements which must all be fulfilled for the classification

- Single pulse criterion

The exposure from any single pulse within a pulse train shall not exceed the AEL for a single pulse.

- Average power criterion

The average power for a pulse train of emission duration T shall not exceed the AEL corresponding to the AEL for a single pulse of duration T . (...) For irregular pulse patterns, T has to be varied between T_i and the time base.

- Pulse train criterion

The energy per pulse shall not exceed the AEL for a single pulse multiplied by the correction factor C_5 . (...) The energy from any group of pulses (or sub-group of pulses in a train) delivered in any given time shall not exceed the AEL for that time.

The first criterion is a special case of criterion 2 for $T = \max(t_{\text{pulse}}, T_i)$, because a continuous evaluation includes the emission time of a single pulse. In addition, criterion 2 is a special case of criterion 3 for $C_5 = 1$. Thus, only criterion 3 has to be evaluated for all times between T_i and t_{base} with the value of C_5 based on an image analysis for each emission time. This temporal analysis has to be performed at the most hazardous position (MHP) and the most critical accommodation state.

The MHP is as close to the reference point as possible. For all sensors a closer distance leads to more VCSELs contributing to the image in the eye, which makes it potentially more dangerous. For symmetry reasons a centered position in front of the sensor at a distance of 10 mm represents the MHP. The accommodation state is considered later on in detail, and set to accommodation to infinity for the first step.

3.4 Simplified Analysis (accommodation to infinity)

3.4.1 Image analysis

As discussed earlier the image analysis describes the determination of the most hazardous position. This is done by variation of the eye accommodation (air equivalent of the eye focal length: $f_{\text{eye}} = [14.5 \text{ mm}, 17 \text{ mm}]$, the array distance, and the size of the apparent source. Such an image analysis must be performed for all possible emission times. The large parameter space makes a full analysis challenging and useful assumptions are required to simplify the analysis.

Figure 3 showed that for a distance of 10 cm with 7 mm aperture (measurement condition 3) not all VCSELs contribute to the total power behind the 7 mm aperture depending on the field-of-view. A shorter distance will result in more power entering the eye which is potentially more dangerous. On the other hand, a shorter distance will result in a blurred image on the retina due to the limited ability of the eye to produce a sharp image at small distances. Finally, a distance $> 10 \text{ mm}$ will result in less VCSELs entering the aperture which is less critical for the image analysis.

The VCSEL array is placed in the focal plane of the optics and thus placed at infinity from the perspective of the viewer. If the viewer accommodates to infinity the retinal image has the same angular distribution as the original emitter array. A single VCSEL with a diameter of $d_{\text{VCSEL}} = 14 \mu\text{m}$ has a beam divergence of

$$\alpha_{\text{VCSEL}} = 2 \arctan\left(\frac{d_{\text{VCSEL}}}{2f_0}\right) \approx \frac{d_{\text{VCSEL}}}{f_0} = \begin{cases} 0.4 \text{ mrad} & 11^\circ \\ 1.2 \text{ mrad} & 32^\circ \\ 2.5 \text{ mrad} & 60^\circ \end{cases}, \quad (9)$$

for the three optics configurations {I, II, III}. This can be compared to the minimal spot size with respect to the standard of $\alpha_{\text{min}} = 1.5 \text{ mrad}$ which shows that for all optics a single VCSEL emits a collimated laser beam (slightly larger for the 60° optics). In the next step, the whole array composed of multiple small sources shall be considered based on the method described in the official IEC interpretation sheet [5]. Table 3 summarizes the angular subtense between VCSELs based on equation (9), where d_{VCSEL} is replaced by the horizontal ($d_H = 50 \mu\text{m}$) and the vertical spacing ($d_V = 40 \mu\text{m}$) between the VCSEL centers.

Symbol	Unit	11°	32°	60°
α_{VCSEL}	mrاد	0.4	1.2	2.5
angular subtense horizontal	mrاد	1.5	4.4	9.1
angular subtense vertical	mrاد	1.2	3.5	7.3
VCSEL in 100 mrad (H)		66	23	12
VCSEL in 100 mrad (V)		82	29	14

Tab. 3: Angular subtense and angular VCSEL spacing in horizontal and vertical dimension

In order to determine what combination of VCSELs is the most critical one a simplified image analysis is applied. In this analysis rectangular image shapes² are considered with varying size. The highest ratio of the accessible emission E_{AE} and the accessible emission limit E_{AEL} defines the critical α dimension of the image analysis

$$\frac{E_{\text{AE}}}{E_{\text{AEL}}} \sim \frac{1}{1000} \frac{n_{\text{H}} \cdot n_{\text{V}}}{\bar{\alpha}} \quad \text{with} \quad \bar{\alpha} = \frac{\alpha_{\text{H}} + \alpha_{\text{V}}}{2} \quad (10)$$

where the amount of VCSELs (proportional to E_{AE}) included in the analysis is adjusted by the numbers $n_{\text{H/V}} \in \mathbb{N}$. The scaling of the accessible emission limit (AEL) is proportional to C_6 and thus proportional to α . $\bar{\alpha}$ is the arithmetic mean between the horizontal and the vertical angular dimension. Both α_{H} and α_{V} are always larger than α_{min} and smaller than α_{max} .

The result of such an analysis is shown in table 4 up to a size of 3 times 3 VCSELs. For example, in case of the 32° optics a sub-array of three horizontal and two vertical VCSELs result in a ratio of 0.82, which is more critical than a single VCSEL with 0.67, but less critical than an array of three times three.

The result of the image analysis depends on the emission time because α_{max} is emission time dependent. In addition, at short emission times not the whole array has been fired. For example, during the activation of the first row only this row must be considered even if α_{max} covers more than one row. In other words, the image analysis is restricted to images smaller than α_{max} but also to the actual amount of rows that were active starting at $t_{\text{emiss}} = 0$. In case the row order is not sequential the image analysis has to be performed for all relevant sub-regions where rows were active.

	11°				32°				60°			
$n_{\text{V}} \setminus n_{\text{H}}$	1	2	3	128	1	2	3	128	1	2	3	128
1	0.67	1.18	1.22	...	0.67	0.56	0.52	...	0.40	0.28	0.26	...
2	1.29	2.29	2.40	...	0.64	0.78	0.82	...	0.32	0.37	0.39	...
3	1.40	2.55	2.90	...	0.62	0.87	0.98	...	0.31	0.41	0.48	...
80	71.58	24.45	11.78

Tab. 4: Image analysis for all field-of-views. For details see text.

In the next step the image analysis above is refined. So far the image analysis was carried out with the same power for each VCSEL. However, as shown in figure 3, this is in particular not true for larger field-of-views. Since

² It is legitimate to consider circular image shapes too, however, the rectangular shape is more restrictive by about a factor of $\frac{4}{\pi}$.

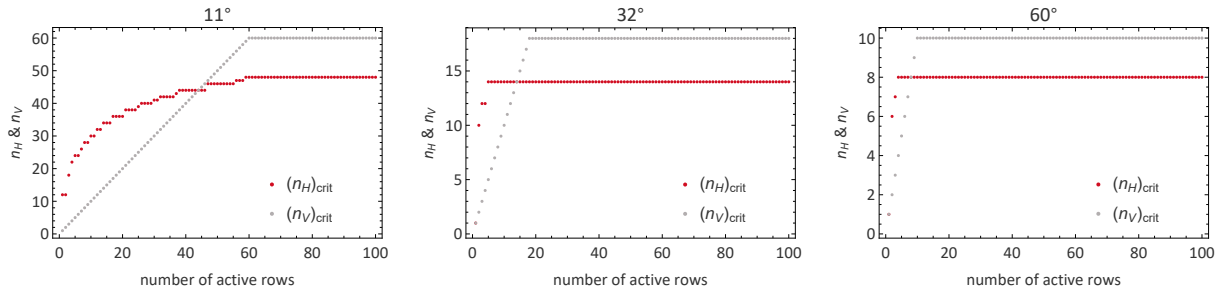


Fig. 5: The figures show the result of the simplified image analysis for all optics, which includes the actual power per VCSEL. The x-axis shows the number of used rows in consecutive order from $t = 0$ s to $t < 40$ ms (1 frame). The red and gray line show the result for of the image analysis. E.g. in case of 11° , when the 5th row is fired, the solution of the image analysis is $(n_H \times n_V)_{\text{crit}} = 24 \times 5$. The analysis is not carried out for $t > 40$ ms, instead the critical number of VCSELs remains approximately constant after the first frame was fired.

VCSELs on the edges contribute less or even nothing to the total power in the eye the accessible emission E_{AE} does not increase further and the ratio becomes not more critical. A numeric analysis which uses the correct spot powers per VCSEL shows that the most critical array sizes are

$$(n_H \times n_V)_{\text{crit}} = \begin{cases} 48 \times 60 & 11^\circ \\ 14 \times 18 & 32^\circ \\ 8 \times 10 & 60^\circ \end{cases} \quad (11)$$

which differs from the original evaluation in table 4 and is less than the maximum amount of VCSELs in 100 mrad. The image analysis can be further generalized for the case when not all rows were fired. The result of the most critical array size depending on the number of fired rows is shown in figure 5 for all optics. For further details refer to the description below the figure.

3.4.2 Temporal analysis

With the simplified image analysis at hand a full temporal analysis can now be performed for each configuration. To determine α , α^* , E_{AE} and E_{AEL} the following scheme is used

1. Choose an emission time $t_{\text{emiss}} \in [t_{\text{pulse}}, t_{\text{base}}]$.
2. Calculate $\alpha_{\text{max}}(t_{\text{emiss}})$ with equation (1).
3. a) α : Perform a restricted image analysis. Horizontal and vertical angular dimensions are bound to α_{max} . n_V cannot exceed the number of fired rows during t_{emiss} . n_H and n_V cannot exceed the limits defined in equation (11).
b) α^* : Perform an unrestricted image analysis with $\alpha_{\text{max}} = 100$ mrad analogously.
4. E_{AE} is defined by the sum over all output energies of the critical VCSELs $(n_H \times n_V)_{\text{crit}}$ based on the restricted image analysis.
5. E_{AEL} is defined by equation (8). C_5 is derived with α^* , T_2 and C_6 with α .

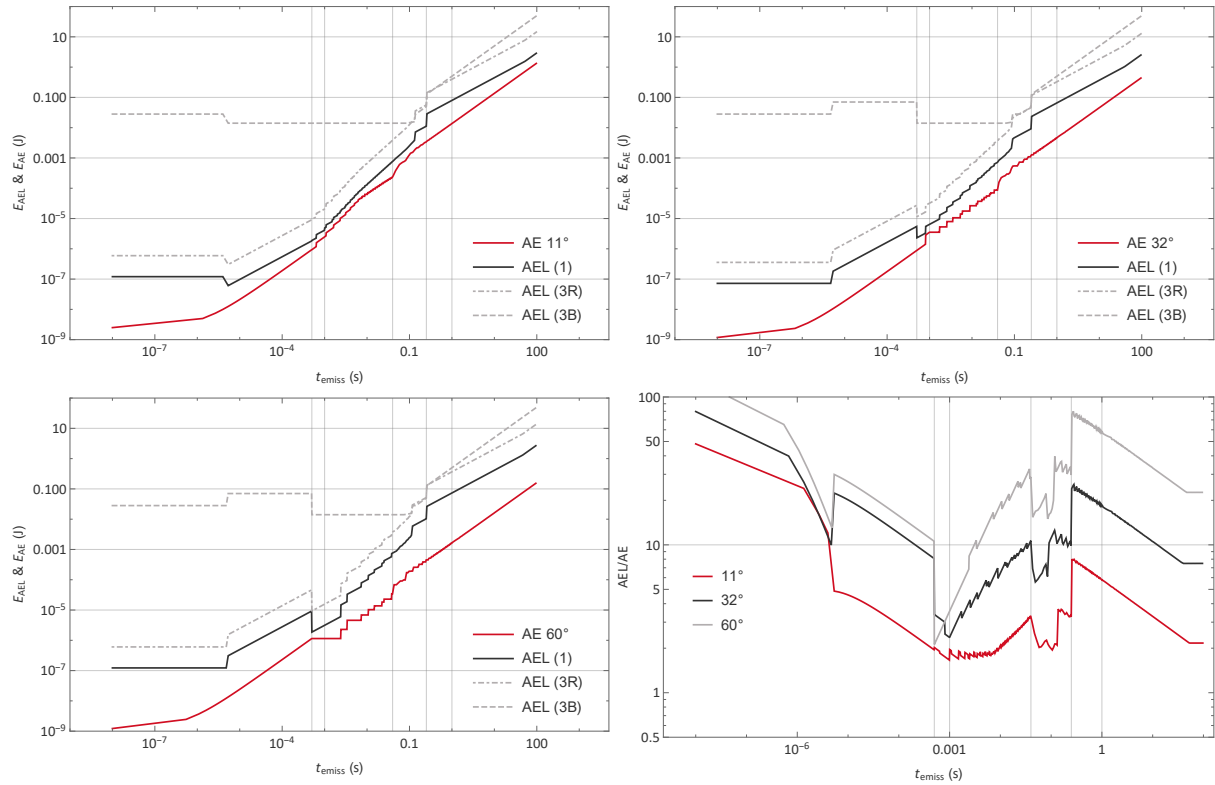


Fig. 6: The first three plots show the simplified analysis for configuration I-III in red based on 1 nJ energy per pulse, the different E_{AEL} for laser class 1 in black, and 3R and 3B in gray. The vertical gridlines indicate the time for the end of one row (500 μs), two rows 1 ms, the end of one frame (40 ms), 0.25 s, and 1 s. The plot on the bottom right shows the ratio between E_{AEL} of class 1 and E_{AE} with the two horizontal gridlines at 1 and 1.25.

6. Repeat steps 1 – 6 for all emission times, e.g. one analysis for each shot.

The temporal analysis is performed for the standard configuration I-III with 128×80 active VCSELs, which is more restrictive than the configuration with 100 rows because the energy is less distributed. The input energy of the analysis is set to 1 nJ which allows for an easy scaling of the plots for all desired input energies. For the row order the most restrictive configuration is chosen. This means, that the first row is the central one with number 50 that contributes the most to the image on the eye, refer to figure 3. From here on, the following row is always the one which contributes the next most: $50 \rightarrow 49 \rightarrow 51 \rightarrow 48 \rightarrow 57 \dots$ This row order is theoretical and will not be used in any sensor configuration, unless a completely randomized row sequence would match this pattern by chance. Nonetheless, it is reasonable to assume this worst case scenario.

The result of the analysis is shown in figure 6 for the three standard configurations I-III based on 1 nJ energy per pulse. In addition, the bottom right figure shows the ratio between E_{AEL} and E_{AE} which corresponds to the safety margin if the value is larger than one. The safety ratios R are

$$R_{\text{simplified}} = \min \left(\frac{E_{AEL}}{E_{AE}} \right) = \begin{cases} 1.66 & 11^\circ \\ 2.37 & 32^\circ \\ 2.12 & 60^\circ \end{cases}, \quad (12)$$

Based on these ratios the acceptable energy can be calculated. Assuming a 25% safety margin the following inequation must be fulfilled for the pulse energy per shot

$$R \times \frac{1 \text{ nJ}}{E_{\text{pulse}}} > 1.25 , \quad (13)$$

which is true for an energy per pulse of 1.3 nJ under worst case conditions (temperature and tolerances).

To demonstrate the calculation procedure in more detail the following example shall be considered for $\Phi_H = 11^\circ$. An emission time of $t_{\text{emiss}} = 1 \text{ ms}$ is chosen which corresponds to the end of the second burst. Based on equation (1) this corresponds to $\alpha_{\text{max}} = 6.3 \text{ mrad}$ for the restricted image analysis. The maximum number of VCSELs that fit in α_{max} is

$$n_H = \left\lfloor \frac{2f_0 \tan(\alpha_{\text{max}}/2) - d_{\text{VCSEL}}}{d_H} \right\rfloor + 1 = 4 , \quad n_V = \left\lfloor \frac{2f_0 \tan(\alpha_{\text{max}}/2) - d_{\text{VCSEL}}}{d_V} \right\rfloor + 1 = 5 , \quad (14)$$

However, until t_{emiss} only two rows were active which is why n_V is restricted to 2. This leads to

$$\alpha = \frac{\alpha_H + \alpha_V}{2} = \arctan\left(\frac{(n_H - 1)d_H + d_{\text{VCSEL}}}{2f_0}\right) + \arctan\left(\frac{(n_V - 1)d_V + d_{\text{VCSEL}}}{2f_0}\right) \approx 3.3 \text{ mrad} \quad (15)$$

where α is defined as the arithmetic mean between α_H and α_V . The same analysis is carried out in the case of the unrestricted analysis. The maximum amount of VCSELs that fit in 100 mrad is shown in table 3. Again, only two rows were fired until t_{emiss} and the most critical image size is given by figure 5 with $(n_H \times n_V)_{\text{crit}} = 12 \times 2$. This leads to $\alpha^* \approx 9.5 \text{ mrad}$.

In the next step the accessible emission is determined. After $t_{\text{emiss}} = 1 \text{ ms}$ each VCSEL of the two rows has fired exactly

$$N_{\text{shot}} = \left\lfloor \frac{500 \mu\text{s}}{T_{\text{shot}}} \right\rfloor + 1 = 375 \quad (16)$$

times, which is multiplied with the number of critical VCSELs (based on the restricted analysis), the shot energy and the numerically calculated correction factor, that accounts for the actual power that enters the eye (compare figure 3)

$$E_{\text{AE}} = 375 \cdot (4 \times 2)_{\text{crit}} \cdot 1 \text{ nJ} \cdot 0.83 \approx 2.5 \mu\text{J} . \quad (17)$$

Finally, the accessible emission limit must be determined, which depends on three correction factors, see equation (8). The first correction factor only depends on the wavelength and is $C_4 = 2.34$. C_6 depends on the restricted image analysis and yields $C_6 = \alpha/\alpha_{\text{min}} = 2.2$. C_5 is calculated with equation (5). Since $\alpha^* > \alpha_{\text{max}}$ and $N = T_2/t_{\text{emiss}} > 625$ the correction factor is $C_5 = 0.2$. In total the accessible emission limit is thus

$$E_{\text{AEL}} = 7 \times 10^{-4} t_{\text{emiss}}^{3/4} C_4 C_5 C_6 \text{ J} \approx 4.1 \mu\text{J} , \quad (18)$$

which corresponds to a safety ratio of about $1.7 > 1$ which corresponds to the graph shown in figure 6 in the bottom right plot.

3.5 Advanced analysis (arbitrary accommodation & row order)

The simplified analysis as described before did not consider different accommodation states that can make the analysis more restrictive. In addition, neither the row sequence nor the shot pattern could be adjusted to an

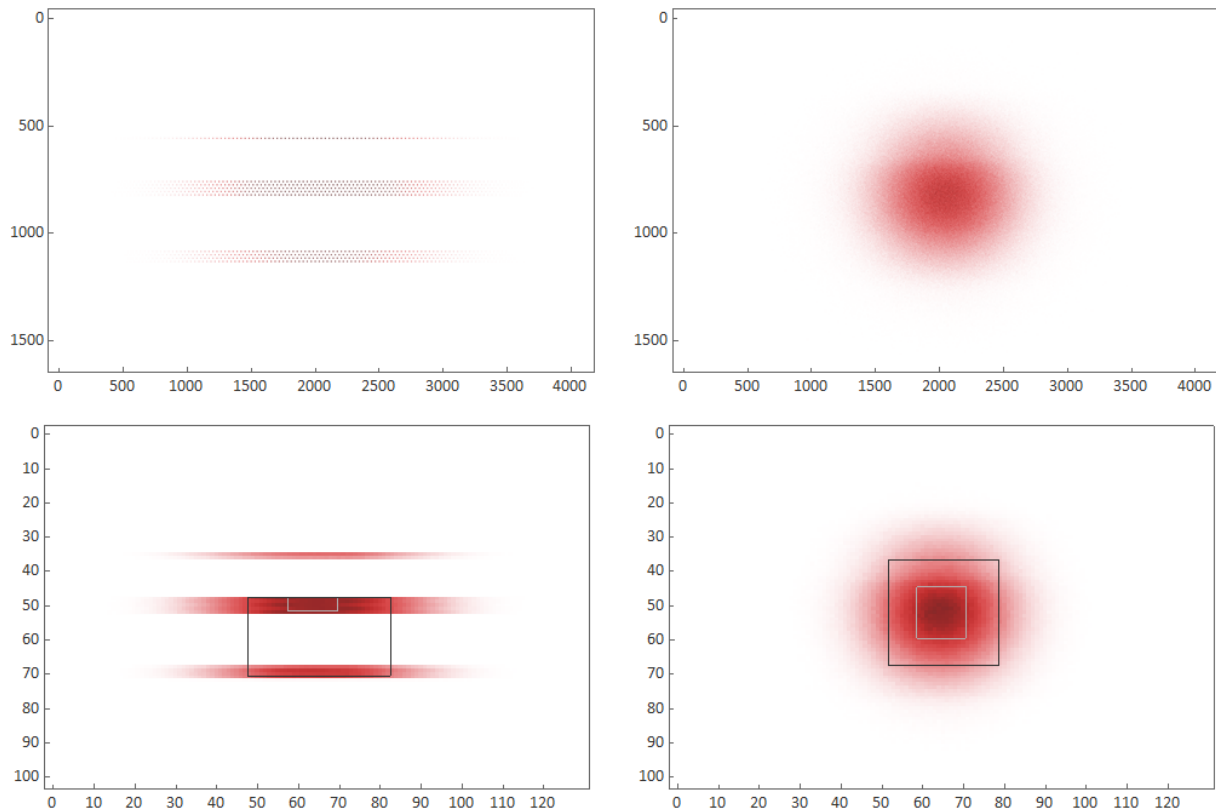


Fig. 7: The top two plots show the resulting image on the retina for two accommodation states with 17.0mm (left) and 14.5mm (right). The axes refer to the sampling resolution of the image on the retina. In both cases the rows 48-52, 69-72, and 35 were fired with the same number of shots. The two plots on the bottom show two image analysis on the downsampled images. The image analysis in gray is limited to $\alpha_{\max}(t_{\text{emiss}})$, here 20mrad, while the black image analysis is limited to 100mrad and is thus used to determine α^* .

arbitrary pattern. All these features are included in the advanced analysis, which is, however, much more time consuming because the image analysis has to be repeated for each point in time, which includes a full Optics Studio simulation.

3.5.1 Image analysis

To account for different accommodation states and arbitrary row sequences an Optics Studio simulation is performed for each point in time. The image on the retina is simulated with a resolution of 4096×1600 . An example is shown in figure 7 in the top two plots for a focal length of $f_E = 17.0\text{mm}$ (accommodation to infinity) and $f_E = 14.5\text{mm}$. To perform the image analysis the image is downsampled to a lower resolution, due to performance reasons in the image analysis algorithm. The image analysis is then performed numerically by finding the most critical ratio $E_{\text{AE}}/E_{\text{AEL}}$, compare equation 10, within the boundaries of α_{\max} .

3.5.2 Temporal analysis

As a first step the advanced temporal analysis is performed for an accommodation to infinity to verify whether the simplified analysis is reproduced. Figure 8 shows the comparison between both methods on the left for all optics, where the dots represent the advanced scheme. Both schemes match quite well with marginal differences. In the next step the accommodation state is varied by changing the focal length of the eye. In the air equivalent the focal length is adjusted between 14.5 mm and 17 mm where the latter corresponds to accommodation to infinity. The resulting safety ratios are shown in figure 8 on the right.

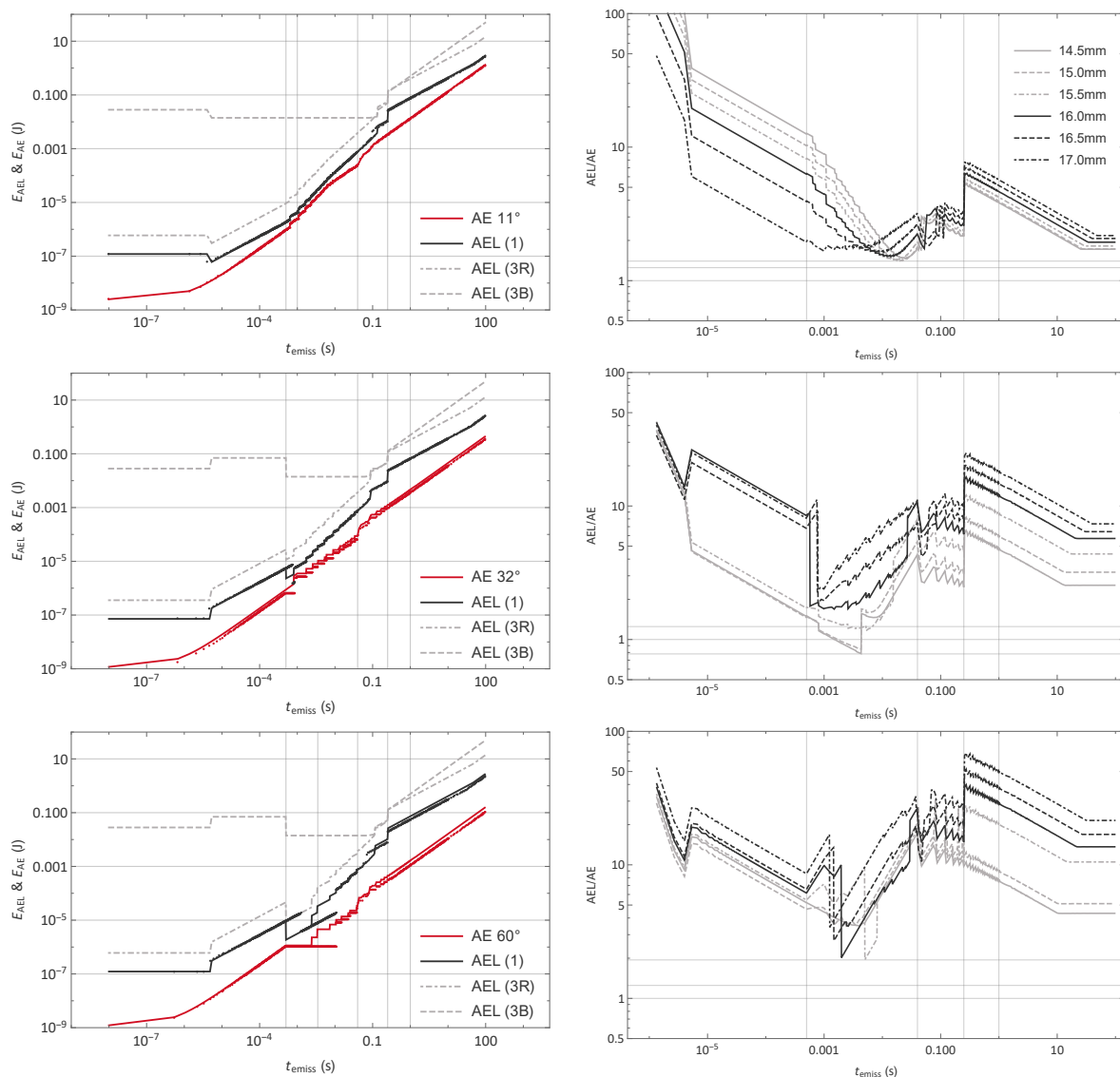


Fig. 8: (Left) Comparison between simplified and advanced analysis for the case of accommodation to infinity for all optics. The result of the advanced analysis is represented by the dots. (Right) The plots show the safety ratio for the advanced analysis. The safety ratio was evaluated for different accommodation states of the eye modeled by the eye's focal length between 14.5 mm and 17.0 mm.

All ratios are more restrictive with the advanced analysis with the largest impact for 32°.

$$R_{\text{advanced}} = \min \left(\frac{E_{\text{AEL}}}{E_{\text{AE}}} \right) = \begin{cases} 1.40 & 11^\circ \\ 0.78 & 32^\circ \\ 1.94 & 60^\circ \end{cases}, \quad R_{\text{simplified}} = \begin{cases} 1.66 & 11^\circ \\ 2.37 & 32^\circ \\ 2.12 & 60^\circ \end{cases}, \quad (19)$$

In addition, it can be clearly seen, that the 32° sensor is the most dangerous one from this selection of field-of-views. The smaller the field of view, the more spots enter the eye. However, a smaller field-of-view also leads to larger beam spots in the near field due to the larger focal length of the optics. For 60° a very limited number of spots enters the eye, but each spot that hits the eye contributes with almost the full power. On the other hand, for 11° a lot of spots enter the eye, but most of them only with a fraction of the original power. 32° is in between those two “extremes” with a considerable number of spots and considerable amount of power per spot, leading to a more hazardous sensor setup.

3.6 Configuration parameters

Based on the final safety ratios R_{advanced} of the advanced analysis the final energy for each configuration can be calculated. Table 5 summarizes all necessary conditions for a laser safe configuration. The pulse energies are provided for different sensor heatsink temperatures based on figure 2 and with/without the additional safety margin of 25%.

Parameter	Symbol	Unit	I	II	III
field-of-view	$\Phi_H \times \Phi_V$	°	11.2 × 5.6	32 × 16	60 × 30
wavelength	λ	nm	885 ± 20		
pulse energy (−40°C)	E_{pulse}	nJ	< 1.40	< 0.78	< 1.94
pulse energy (+60°C)	E_{pulse}	nJ	< 1.17	< 0.66	< 1.62
pulse energy (−40°C) (incl. 25%)	E_{pulse}	nJ	< 1.13	< 0.62	< 1.55
pulse energy (+60°C) (incl. 25%)	E_{pulse}	nJ	< 0.93	< 0.52	< 1.30
number of shots	n_{shot}	1	≤ 374	≤ 749	≤ 936
shot period	T_{shot}	μs	> 1.334	> 0.667	> 0.534
frame rate	f_{frame}	Hz	≤ 25		

Tab. 5: The table summarizes the necessary conditions for a laser safe configuration. The temperature refers to the heatsink temperature of the sensor. The allowed energies are calculated with and without the additional 25% safety margin. The values at 60°C are calculated from an extrapolation based on the data of figure 2

One important property of the laser safety analysis is the fact that the calculation is invariant (to first order) when the pulse energy and the number of shots are adjusted at the same time in opposite direction. For example, if the pulse energy is increased by a scaling factor of 2 and the number of shots is reduced by the same factor of 2, the outcome of the analysis is the same for sufficiently large emission times, because the average energy per time stays the same. In addition, the result of the analysis is also unaffected for short emission times if the

scaling factor is below 10, because the AEL for a small number of pulses is more than one order of magnitude higher than the AE, see figure 8.

4 Single-fault condition

4.1 Critical parameters

The next step is the analysis of the sensor system in the presence of errors that cause an abnormal operation. The laser safety standard [1] defines the test conditions for the determination of the accessible emission level and specifies that

DIN EN 60825-1:2015-07 – §5.1

Tests shall take into account all errors and statistical uncertainties in the measurement process and increases in emission and degradation in radiation safety with age.

In addition, it is necessary to ensure that

DIN EN 60825-1:2015-07 – §5.1

The above tests shall be made under each and every reasonably foreseeable single-fault condition. However, if the emission is reduced to a level below the AEL by automatic reduction in a duration within which it is not reasonably foreseeable to have human access, then such faults need not be considered.

The main parameters which are critical for laser safety are

- pulse power → more power leads to more energy per shot which is critical for laser safety
- pulse width → a longer pulse with the same power leads to more energy which is critical for laser safety
- time between shots → a shorter time between subsequent shots leads to more energy per time which is critical for laser safety
- row sequence → adjacent rows are more critical for laser safety

Additional parameter, that also have an influence on the classification are

- field of view
- frame rate
- number of rows
- number of columns

However, these are assumed to be constant, or (in case of the frame rate) are already indirectly included in the parameters of the first list. The general concept is based on monitoring of all critical parameters and to detect any deviation from the intended operation. Therefore, appropriate monitoring functions must be foreseen in the system with sufficiently short reaction times.

4.2 Component requirements

The three main components that are relevant for laser safety are the Ibeo NEXT Laser Driver (INLD), the Ibeo NEXT Receiver ASIC (INRA) and the Ibeo NEXT VCSEL (INVCSEL). INLD and INRA are both designed with several monitoring functions to ensure an operation according to the defined configuration. These shall be discussed in the next sections. Limitations that are only present during specific component samples are indicated as such by e.g. INLD.A0 for the A0-sample of the INLD.

4.2.1 INLD

The requirements of the INLD are found in the Ibeo Next Laser Driver Spec [6], with the errata sheet [7]. In the following section laser safety relevant requirements shall be discussed.

INLD8101

The INLD ASIC (Driver IC) shall ensure that the output current is not violating the defined specification (acc. to INLD7433 and INLD0500) for the Pulse width by more than ± 2 ns plus a configurable value.

⚠ Available with reduced resolution for INLD.A0-sample. Based on the currently available information the monitoring accuracy is limited to a resolution of ± 6.4 ns (300 MHz clock) which allows for higher variations than the laser safety margin.

INLD8102

The INLD ASIC (Driver IC) shall ensure that the output current does not deviate from the configured output current (specified in INLD7434 and INLD0450) by 20% but at least ± 600 mA.

⚠ Not available for the INLD.A0-sample.

INLD8103

The maximum amount of laser pulses within a 10 second period shall be monitored with an accuracy of 10%.

Not directly required for laser safety. Can be used as consistency check. However, the “integration time” of 10 s is too long to provide monitoring functionality.

INLD8104

The INLD shall monitor the VCSEL row voltage and detect when more than 20% of emitters per row resemble an electrical open or short (INLD_FSR_2.4).

⚠ Not available for INLD.A0-sample.

INLD8105

The time between two current pulses within one laser shot cycle shall be monitored and checked against a lower limit (RG_SAFETY_TIME) with an accuracy of < 100 ns. Every row group shall have its own value stored in a configuration register RG_SAFETY_TIME[0..9] and a violation shall trigger the laser safety error mechanism, i.e. a transition to ErrorSafetyMonitor, that can be masked with the bit EYE_SAFETY in the register SAFETY_MASK (INLD_FSR_2.3).

⚠ Not available for INLD.A0-sample.

INLD8140-INLD8148

The laser emission shall be monitored per row. There shall be a 40-bit unsigned counter for every row, representing the accumulated emitted laser energy within a time window. (...)

⚠ The monitoring function is used during all sample phases to monitor the active time of each row and the equivalent total number of shots per row. Each shot increments the safety counter weighted by the pulse width and the pulse height. During INLD.A0-sample these two values are constants, during INLD.B0 the values are based on the current and width measurement. The decrement is configured such that each row counter drops down to zero just before the row is fired again in the normal configuration. The safety threshold is configured slightly higher than the maximum safety counter number of each row during normal operation.

4.2.2 INRA

The DigitalDesignSpec for the INRA contains several requirements relevant for laser safety [8]. In the following section laser safety relevant requirements of the laser monitoring unit (LMU) shall be discussed. FIREBIRD is the paraphrase for the INRA.

DDS_FIREBIRD_0186

The LMU of FIREBIRD device perform monitoring for critical timings related to eye safety.

DDS_FIREBIRD_0186

This sub-system shall detect error and react as fast is possible to perform the following operation: 1) Force the VCselOFF pulse to enable state. 2) Disable the communication of the SPI Laser driver interface by forcing to high state all chip select signals. 3) Force in mute the Measurement control.

⚠ The hardware/software reaction times are not yet known and should be investigated with the first samples.

DDS_FIREBIRD_0189

The Laser driver sub-system shall program at the beginning of each ROW cycle the emitter unit external device. If start pulses are detected during this programing time, the LMU shall raise an error.

This functionality ensures that the shot sequence of each row does not start during the programming time of each row.

DDS_FIREBIRD_0190

The LMU shall monitor the pulse width of laser_on_pulse

This functionality monitors the laser pulse width of each individual shot with 0.25 ns stepsize, which exceeds the potential of the INLD. This measurement is either based on the start and stop signals (indirect measurement, fast), or on the sense signals (direct, slower). The second option should be preferred if the reaction times are sufficiently small. A potential variation due to the measurement from shot to shot must be evaluated.

DDS_FIREBIRD_0191

The LMU shall monitor the start pulse occurring into a time window. The window of the start pulse detection is define from the shot sync event generated by the measurement control sub-system

This ensures, that a start pulse cannot occur outside the predefined shot window.

DDS_FIREBIRD_0193

The LMU shall accumulate the laser on time occurring into the window.

This monitors the total number of shots during each cycle, and raises an alarm if the number is too high.

DDS_FIREBIRD_0195

The LMU shall monitor the shot cycle.

This monitors the time between subsequent shots and raises an alarm if the time is too long or too short.

In summary, the INRA is able to monitor the pulse width and the time between subsequent shots. In addition, it receives a feedback signal from the INLD for the row switch which can be used to monitor the row number. The only information not available to the INRA is the pulse power.

4.3 Safety Assurance

The following section discusses reasonably foreseeable hardware or software single fault errors and their impact on the laser safety concept, as well as manufacturing tolerances and variations.

4.3.1 Pulse power

- **Current source (INLD) and emitter (INVCSEL) variations**

Due to the manufacturing process not all current sources operate at the same design current of 6A. The specified tolerance is between 5.4A and 6.6A [6]. In addition, the INVCSEL components have a different power conversion efficiency. **Each transceiver module must be tested such that the pulse energy at -40°C junction temperature at an equivalent of 6.6A is less or equal to the pulse power of the laser safety**

calculation.³

Note, that an INLD.A0 operating at 5.4A can be matched to an INVCSEL such that the pulse energy is 1.3 nJ. While such a configuration is safe under standard operating conditions any error that causes a current of > 6.7A would result in a pulse energy which exceeds the 25% safety margin included in the calculation. That's the reason why 1.3 nJ must be achieved at an equivalent of 6.6A. This condition would be violated by a component composition that delivers 1.3 nJ at 5.4A.

- **Row-to-row emitter variation** Due to the row-wise hardware design not all VCSELs receive the same amount of current. Typically, the first VCSEL of a row, which is closest to the bond wire, has an up to +40% higher optical output [9] than the mean of the row. On the other hand, the two adjacent VCSELs on the row above and below have an up to –25% lower optical power which evens out the high power in between. In addition, this extreme cases are only present on the edges of the VCSEL array which is much less critical than in the center.
- **Short in current source (INLD)**
In case of a short in one of the current sources a maximum current of 7.8A is achievable.
→ **INLD.A0:** If the pulse power at an equivalent of 6.6A during normal operation does not exceed the specified pulse power (see previous point) an operation at 7.8A is an increase of less than 20% which is included in the safety margin.
→ **INLD.B0:** The B0 driver is able to detect a short in the current source within the time between two shots and the laser emission is disabled.
- **Short in multiplexer (INLD)**
A short in a multiplexer is detected by the supply monitoring function of the INLD and laser emission is disabled
- **Bypassed INLD**
Theoretically, the INLD could be bypassed by a metal short which connects one of the pads of the current sources to one of the VCSEL rows. In that case this row would be operated with 300 mA DC.
→ **INLD.A0:** This error is not detected by INLD. However, it is basically impossible to connect the input INLD pins with the output pins by accident. A candidate to create such a bypass would be a loose bonding wire. However, none of the installed bonding wires has sufficient length to connect any current source pad with a VCSEL pad.
→ **INLD.B0:** This error is detected by INLD, reported to the INRA and to the Device Safety & Security Controller, which deactivates the supply.
- **Damaged VCSELs**
Over the lifetime more and more VCSELs are damaged which results in a reduced laser emission. It is not fully analyzed yet whether a damaged VCSEL represents a short or a large resistance. Assuming the worst

³Based on the design specifications of INLD and INVCSEL it's possible that a high performing driver (high output current) is matched to a high performing emitter (high power conversion efficiency) which in combination leads to a pulse energy that is higher than the laser safety limit. This is a necessary consequence to increase the yield of both components during the manufacturing process, and makes a characterization measurement inevitable.

case, the current increases on the remaining VCSELs relative to the number of damaged VCSELs

→ **INLD.A0:** An increased current due to damaged VCSELs up to 25% is covered by the safety margin. A higher amount of damaged VCSELs will be detected by the functional availability which is dramatically reduced when more than 25% of the VCSELs are inoperable.

→ **INLD.B0:** The INLD detects when more than 20% of the VCSELs per row are damaged.

4.3.2 Pulse width

- **Pulse width measurement resolution (INLD)**

The pulse width measurement is limited by the internal measurement resolution. Depending on this resolution significant changes compared to the configured value can remain undetected.

→ **INLD.A0:** The resolution is limited to ± 6.4 ns which is in the order of the actual pulse width and thus not sufficient to ensure laser safe emission. However, the feedback signal of start and stop pulse is measured with an accuracy of 0.3 ns and transmitted to the INRA which monitors the pulse width. For pulse widths > 4 ns a change of 0.6 ns is less than the 25% safety margin and thus safe to operate.

→ **INLD.B0:** The resolution is ± 1 ns which can be sufficient depending on the configured pulse width. Small deviations are still monitored and reported by the INRA, while larger deviations are also covered by the INLD.

4.3.3 Row sequence

- **Pulse power integrator (INLD)**

The total number of shots per row is a pulse power integrator which increments after each shots. If more shots are fired than configured the accumulated number reaches a threshold and the laser emission is disabled.

→ **INLD.A0:** The increment is weighted by the configured pulse power and width. Thus, each shot contributes with the same value independent of its actual power and width. However, these two parameters are individually accounted for and the pulse power integrator can still be used to monitor the active time of each individual row. This ensures that no row is fired twice during one frame.

→ **INLD.B0:** The integrator uses the measured pulse power and width which allows for a more advanced monitoring.

- **Loose bonding wire**

A bonding wire that connects e.g. driver output 50 to row 50 and is loose on the VCSEL side could create a connection to a neighboring row. That would lead to configuration where driver output 50 and e.g. 49 are both connected to the same row 49. In consequence, this row would fire two times which cannot be monitored by any device. However, all configurations are calculated such that the double number of shots is safe to operate.

4.3.4 Time between shots

- **Shorter time between shots** A shorter time between two subsequent shots does not necessarily lead to an unsafe operation if the total number shots remains the same. If, however, the total number of shots

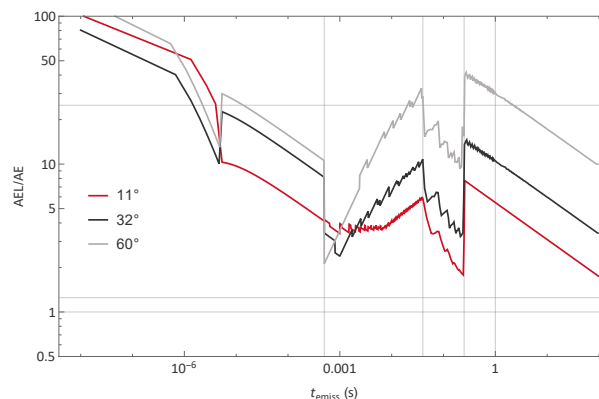


Fig. 9: The plot shows the safety margins for the closest point of human access based on a single pulse energy of 1 nJ. The AEL values are for a laser class 1 device.

changes by more than 25% this configuration becomes critical. In addition, for very short times between shots the configuration can also become critical.

→ **INLD.A0**: No functionality is included in the INLD to measure the time between shots. The INRA is, however, fully capable to monitor the time between shots with sufficient time resolution.

→ **INLD.B0**: In addition to the INRA also the INLD performs a direct monitoring of the time between shots.

4.3.5 Configuration

- **Flash of faulty configuration** Any configuration that is flashed on a release version of the sensor must have been approved with by laser safety. Laser safety class 1 is only ensured for approved configurations. Internal sensor diagnostic ensures that the configuration is flashed correctly.

5 Hazard analysis

5.1 Closest point of human access

According to the standard [1] the closest point of human access must be considered as well with a modified measurement condition

DIN EN 60825-1:2015-07 – §7.3

For Class 1 (...), if the accessible emission exceeds the AEL of Class 3B as determined with a 3.5 mm diameter aperture placed at the closest point of human access, an additional warning shall be given on a product label and in the information for the user (...).

To cover the worst case, the analysis is performed without an installed front cover. The array-to-eye distance for the three optics are 44.168 mm, 44.975 mm and 39.345 mm for 11°, 32° and 60°.

The analysis is equivalent to the simplified analysis in section 3.4. However, the input based on figure 3 and 5 is adjusted accordingly. The result of this analysis is shown in figure 9. All sources are well below the safety

limits of class 1. Compared to class 3B the safety margins are

$$R = \min \left(\frac{E_{AEL}^{3B}}{E_{AE}} \right) = \begin{cases} 5.86 & 11^\circ \\ 11.21 & 32^\circ \\ 32.96 & 60^\circ \end{cases} . \quad (20)$$

Thus, the sensor poses no threat even at very close distances to the eye or the skin in the standard configuration.